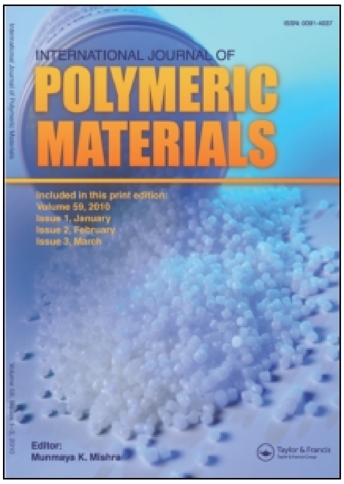

International Journal of Polymeric Materials
Publication details, including instructions for authors and subscription information:
http://www.informaworld.com/smpp/title~content=t713647664

Analysis of Polarized Light Scattering from Solid Polymers by Optical Modeling

Ivanka T. Moneva

To cite this Article Moneva, Ivanka T.(2002) 'Analysis of Polarized Light Scattering from Solid Polymers by Optical Modeling', International Journal of Polymeric Materials, 51: 1, 193 — 207
To link to this Article: DOI: 10.1080/00914030213026
URL: http://dx.doi.org/10.1080/00914030213026

International Journal of Polymeric Materials, 51:193 – 207, 2002

0091-4037/02 $12.00 + .00

Analysis of Polarized Light Scattering from Solid Polymers by Optical Modeling*

IVANKA T. MONEVA[†]

Institute of Polymers, Bulgarian Academy of Sciences, Sofia, 1113 Bulgaria

(Received 5 March 2001; In final form 10 March 2001)

The basic principles and use of the optical modeling method in the analysis of non-isotropic light scattering from solid polymer systems have been outlined. The concept considered extends the method of the optical Fourier transforms assuming analogy between polarized light scattering from anisotropic samples and nonpolarized light diffraction at isotropic samples. The experience in construction of optical models for certain morphological types in solid polymers and their use to study inter-particle interference effects upon scattering is resumed. New potentials of the optical modeling are revealed in its interaction with the method of digital image analysis.

Keywords: Polarized light scattering; Optical modeling; Polymer solids; Interparticle interference; Computer simulation

INTRODUCTION

The method of polarized light scattering (PLS) is usually applied to study the morphology in polymer solids on the scale of several microns [1 – 3]. The method is relatively easy to use with regard to its instrumental basis. Even a conventional polarizing microscope can be in use to obtain and record the scattering patterns of the objects under study. The interpretation of recorded scattering, however, is sometimes very

---

[*] The paper has been presented at PolyChar'9 World Forum on Polymer Applications and Theory, Denton, Texas, 2001. It is dedicated to Professor S. Fakirov in favour of his 65th birthday.

[†] Fax: 00359 (2) 707 523, e-mail: itmoneva@bas.bg

difficult. The tendency is even enhanced since many new materials with complex morphology have been developed in recent years.

Among the means to help the analysis of scattering is the method of optical modeling. It was created by Bragg in 1939 for analysis of X-ray scattering [4], and is known also as the method of optical analogs, optical Fourier transforms or optical Fourier transformation and optical diffraction, all the terms assenting on its basic features [5–9].

The use of optical modeling to PLS relies on its advantages, among which are the opportunity to study easily the separate role of different factors upon scattering and its direct association with the physical nature of phenomena. Its use in the analysis of PLS from anisotropic samples is based on the fact that the analytical description of scattering by electro-magnetic radiation is, in principle, similar *i.e.*, independent of wavelength.

The optical modeling differs from other modeling methods in the type of models used and in the way of obtaining the intensity distribution of scattered light. The method of optical modeling includes generation of a model (an optical analog) that describes the optical structure of the object, recording a Fraunhofer diffraction pattern at the model and comparison of the diffraction pattern obtained (the optical transform) with the experimentally observed scattering pattern of the object. Alike the other modeling methods, identity of patterns occurs if the right model is taken, even though the model might not be unique.

In this paper, the basic principles for generating optical analogs needed to model the polarized light scattering from anisotropic samples are outlined. The optical analogs of several morphological types in polymer solids and their optical transforms are summarized. An example of the application of the optical modeling to study interparticle interference effects upon scattering is described. The interaction of the optical modeling method with the computer simulation of PLS by digital image analysis is discussed.

OPTICAL ANALOGS OF POLYMER STRUCTURES AND THEIR TRANSFORMS

The concept behind the optical modeling of PLS is straightforward: one is looking at patterns of projections of optical anisotropy and/or optical axis orientation fluctuations of crystallites represented by transparency fluctuations [10–15].

For the purpose of optical modeling we will refer to the basic equation of the PLS method, although its scientific background is classical [1]. The amplitude F_S of light scattered by an isolated homogeneous spherulite having different radial α_r and tangential α_t polarizabilities is given in terms of Rayleigh-Debye-Gans (RDG) approximation by [1]:

$$F_S = K \int_V (\mathbf{PO}) \cos [k(\mathbf{rS})]\, dV. \tag{1}$$

Here **P** is the polarization induced by the electrical field of the incident linearly polarized light in an anisotropic unit volume positioned at distance r from the spherulite center, **O** is the unit vector of the linearly polarized component of scattered light transmitted through the analyzer, $\mathbf{S} = \mathbf{S}_0 - \mathbf{S}_1$ is the difference between the unit vectors of incident and scattered light, k is the wave number and K is a device constant.

Equation 1 can be rewritten in a more general form:

$$F_S = K \int_V (\mathbf{PO}) \exp [-2\pi i(\mathbf{rS})]\, dV. \tag{2}$$

Thus, the scattering amplitude Fs is shown to be to a good approximation the classical Fourier transform of the function (**PO**) which describes the scattering power of the unit volume dV of the spherulite.

Consequently, the optical analog of the spherulite should have transmittance distribution according to (**PO**). The function (**PO**) depends on the optical anisotropy $(\alpha_t - \alpha_r)$ and the state of light polarization, and is given by [1]:

$$(\mathbf{PO}) = E_0\alpha_r \cos\beta + E_0\alpha_t \sin\beta, \text{ at Vv} - \text{polarization and} \tag{3}$$

$$(\mathbf{PO}) = E_0(\alpha_t - \alpha_r) \sin\beta\cos\beta, \text{ at Hv} - \text{polarization.} \tag{4}$$

Here E_0 is the incident field and β is the angle between the polarization direction of incident light and the line connecting a unit element of the scattering area with the spherulite center, it has values from 0 to 360°.

Assuming that E_0 and $(\alpha_t - \alpha_r)$ are constant for all unit elements, the distribution of transparency T for generating analogs of the scattering quasi plane spherulites should be [11–15]:

$$T_{Vv} \sim \alpha_r \cos\beta + \alpha_t \sin\beta, \text{ at Vv} - \text{polarization, and} \tag{5}$$

$$T_{Hv} \sim \sin\beta \cos\beta, \text{ at Hv} - \text{polarization.} \tag{6}$$

In the case of $\alpha_t \ll \alpha_r$ (as for PE), Eq. (5) is simplified:

$$T_{Vv} \sim \alpha_r \cos\beta. \tag{7}$$

The models used were prepared photographically as negative images of drawn patterns with contrast distribution approximately according to Eqs. 6 and 7. The diffraction from the models was recorded in coherent light diffractometer without polarizing elements, the incident light had $\lambda = 700\,\text{nm}$ and degree of partial coherence $\lambda_{12} = 0.5$. The single-spherulite models were of 0.5 mm size that corresponds to maximum intensity reflection at $6'$ [11–14].

Figure 1 shows the optical analogs and the optical transforms of different spherulitic structures: No. (1) a nondeformed spherulite at Hv-diffraction, No. (2) a non-deformed spherulite at Vv-diffraction, No. (3) a deformed spherulite at Hv-diffraction, No. (4) a deformed spherulite inclined to the optical axis of the film at Hv-diffraction, and No. (5) a "ringed" spherulite at Hv-diffraction. The shaded area in the models involve phase changing filters (mica plates) of $\lambda/2$.

The diffraction patterns obtained from the models under Nos. 1 and 2 are completely equal to the familiar PLS patterns of a nondeformed spherulite, respectively, at Hv- and Vv-polarization [1–3] thus implying that the models are correct. The other diffraction patterns are also very similar to relevant scattering patterns from real polymer films containing deformed and "ringed" spherulites [16, 17]. The central spot in the pattern of the deformed spherulite inclined to the optical axis (No. 4) has been observed experimentally [18, 19]. It appears whenever the axis of deformation of an anisotropic structure does not coincide with the plane of polarization of one of the polaroids and can be used to measure photoelasticity [18].

The similarity of the scattering from the 2-dimensional (2-d.) single-particle models to the scattering from the real object can be explained

No.	System	Model	Diffraction	Remark
1	H_{υ}	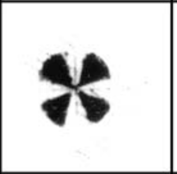		
2	V_{υ}	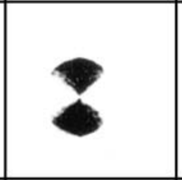	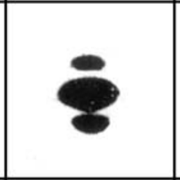	
3	H_{υ}	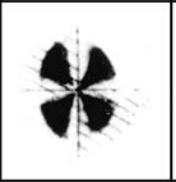	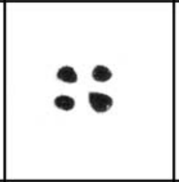	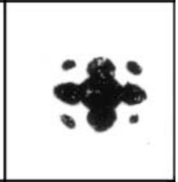
4	H_{υ}			
5	H_{υ}			

FIGURE 1 Optical analogs of scattering spherulitic structures and their optical transforms (see text).

by the fact that the 3-dimensional (3-d.) volume filling spherulites have almost the same scattering envelope under validity of the RDG approximation like the 2-d. ones [20]. Moreover, in cases of random distribution of particles in the solid and/or difference in their size, form and internal structure, the scattering from many particles is well approaching the single-particle scattering [7].

The remarks to Nos. 1 and 3 (Fig. 1) display transforms which were obtained without phase filters. They obviously do not resemble the relevant experimental patterns. The need for introducing phase filters in the models stems from the analysis of (**PO**) given by Eqs. 3 and 4. While (**PO**) at Vv-scattering is always positive (Eq. 3), (**PO**) at Hv-scattering (Eq. 4) can have both positive and negative values because of the different sign of the function $\sin\beta \cdot \cos\beta$ in dependence on the position of the scattering units in the spherulitic particle. Thus, to account for this difference in the case of Hv-scattering, it is necessary to change the phase (in π step) in any two opposite quadrants of the Hv-spherulitic model (shaded in the models Nos. 1 and 3 in Fig. 1)

The physical reason for the additional phase shift needed in optical modeling of non-isotropic scattering is the action of the analyzer. This was revealed considering the compensation of light scattered about the origin by a spherulite [18] and is related to the direction of induced dipols in the scattering units and the sign of their projections along the polarization direction of the analyzer.

It might be of interest to note that due to the phase shift applied in nonisotropic scattering, the effect of the photographic emulsion as a phase object in coherent optical systems [21] is evidently negated. Specifically in the case of Hv-polarized light scattering, the π phase difference appearing is much greater than any other phase difference that could arise from the photographic emulsion. Some effect of the photoemulsion could be expected only in the fine details of the scattering patterns which will be later discussed.

OPTICAL MODELING OF INTERPARTICLE INTERFERENCE

Although many solid polymers are believed to exhibit single-particle type of scattering, interparticle interference can sometimes take place and affect the parameter evaluation based on single-particle scattering theory. Such effects can arise because of the size of particles and their close packing in the solids. They are especially of importance when coherent optical systems of good resolution are involved in the object characterization. Most studies of the interparticle interference effects on PLS so far [22–24] made use of computation of scattering from assemblage models having relatively small statistics. The method of optical modeling allows to study the problem on assemblages with great number of particles and to make an estimate of the interparticle interference effects.

The fundamental equation for the intensity of the electromagnetic radiation I(S) scattered by an assemblage of identical particles in direction S expresses it by means of the scattered intensity by a single particle $I_0(S)$ and an interference factor G(S), which describes the interparticle interference [5–7]:

$$I(S) = I_0(S) \cdot G(S), \tag{8}$$

where $S = (2/\lambda)\ \sin(\theta/2)$, λ is the wavelength of radiation in the scattering medium and θ is the angle of observation.

By introducing the scattering amplitude $F_0(S)$ of a single particle, the intensity $I_0(S)$ is given by:

$$I_0(S) \sim |F_0(S)|^2. \tag{9}$$

By analogy, the interference factor G(S) is given by:

$$G(S) \sim |B(S)|^2, \tag{10}$$

where B(S) is the scattering amplitude of a set of points related to the function A(r), which describes the location of the particles in the object [7].

Thus the scattering amplitude of many particles F(S) is given by the expression:

$$F(S) = F_0(S) \cdot B(S), \tag{11}$$

which allows to model particle assemblages and to study separately the role of the interparticle interference.

The interspherulite interference effect is illustrated here for the case of Vv-scattering because the modelling of Hv-scattering of an assemblage is more difficult. But the results obtained will be in principle valid also in the case of Hv-scattering since the interference function does not depend upon polarization conditions. Therefore, to obtain the scattering amplitudes F(S) and B(S), optical models were generated that combined the V-models of single sperulites located in a given manner. Figure 2 shows the Vv-models of an assemblage with spherulites arranged like the molecules in a liquid (Fig. 2a) and of their centers (Fig. 2b) . Figures 2c and d display the resulting diffraction patterns, respectively I(S) and G(S).

Examples of Vv-models of different assembages, their diffraction and interference patterns are summarized in Figure 3. The models differ in the spherulite size (ds), distance of the closest approach (d_{12}) for a pair of spherulites, the number of scattering spherulites (N) and the packing density (Ω/S_a), where Ω is the surface occupied by all spherulites and S_a is the whole illuminated surface. The numerical values of the parameters for the different assemblages are given in Table I.

By changing the spherulite arrangement, an estimate can be made whether the interspherulite interference has an influence on the

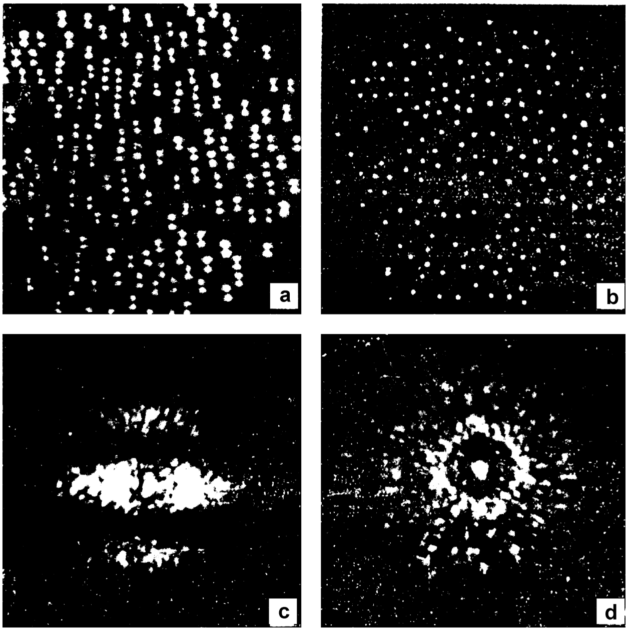

FIGURE 2 Vv-models of assemblages: (a) of spherulites with random distribution and (b) of their centers; and optical transforms: (c) I(S) of the spherulitic assemblage and (d) G(S) of the spherulite centers (see text).

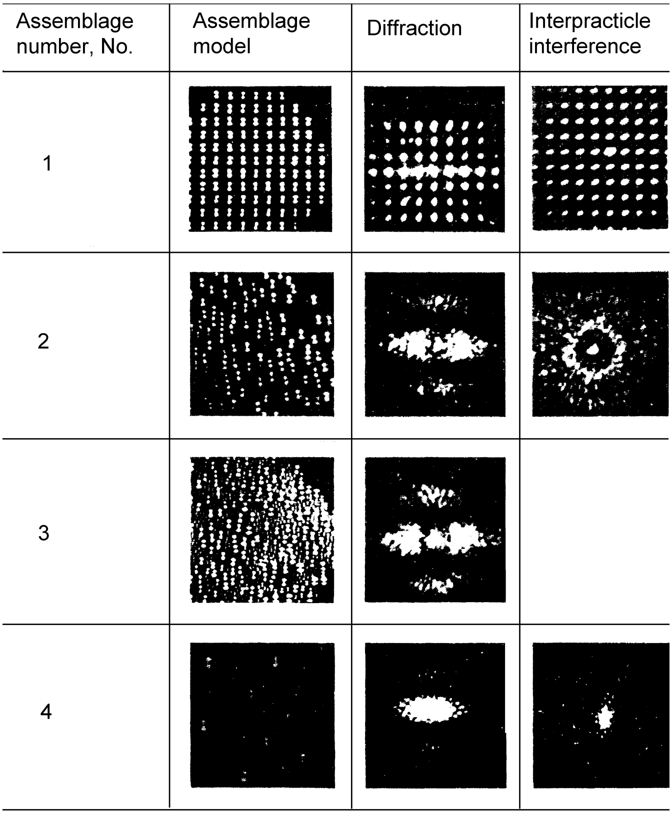

FIGURE 3 Vv-models, Fraunhofer diffraction patterns and interparticle interference patterns for spherulitic assemblages: No. (1) of regular crystalline arrangement, No. (2) liquid-like arrangement of identical particles, No. (3) liquid-like arrangement of polydisperse particles, and No. (4) independent scattering by identical particles.

TABLE I Characteristics of model spherulitic assemblages (see text)

Assemblage number	d_s (*mm*)	d_{12}/d_s	N	Ω/S_a
1	0.5	< 3	126	0.22
2	0.5	< 3	163	0.28
3	0.5	< 3	163	0.42
	0.2	> 3	767	
4	0.2	> 3	12	0.02

diffraction pattern. The assemblages are given regular and irregular (amorph) arrangement, including a regular crystalline arrangement in 2-d. lattice (No. 1), liquid-like arrangement (Nos. 2 and 3) and an approach to "solid body of gaseous type" (No. 4). The latter model is constructed taking into account that particles scatter independently when $d_{12} \gg \lambda$ and $d_{12}/d_s > 3$ [25].

The main feature of the optical analogs shown in Figure 3 is their resemblance to the single-spherulite Vv-scattering pattern while differing in the fine structure, which is discrete. The interparticle interference patterns obtained show the known interference effects of sharp point reflexes (No. 1) and diffraction halo (Nos. 2 and 3) resulting from a crystalline lattice and from liquids, and smoother halo with polydisperse systems (No. 3) [8]. A comparison of the assemblage patterns with the interference patterns clearly shows that the discreteness of all assemblage patterns is due to the interspherulite interaction. Scattering patterns of spherulitic objects obtained by correlation analysis have shown similar modulations of the intensity envelope what confirms the results of the optical modeling [26].

The redistribution of the intensity of the scattering patterns of the assemblages as a result of the interparticle interference could influence the angular position of the maximum intensity reflex $\theta_{\max}$ at Hv-scattering by a single spherulite being used to determine the spherulite size. An estimate can be obtained by comparison of the maximum intensity reflex θ_h (from the interference pattern) with the expected value of $\theta_{\max}$ for a single spherulite. For instance, for the assemblage No. 2 in Figure 2 no effect is expected since $\theta_h = 4' < \theta_{\max} = 6'$. As seen also, the interference ring (the halo) does not cross the meridional reflections of the assemblage Vv-pattern, which result mainly from the anisotropic component of single-spherulite scattering [1]. The interference effect on the Hv-scattering probably depends both on the kind of the interference function and the function of radial intensity distribution of scattered light by a single particle.

It is of interest that even the pattern of independently scattering spherulites (No. 4) is discrete. This obviously can be referred to the s.c. speckle phenomenon, a result of random interference [27, 28], with many applications in experimental mechanics. Some possible applications based on the speckle created in PLS are extended to perform strain analysis of polymers and polymer composites [3, 29].

COMMENTS ON DIGITAL IMAGE ANALYSIS AND OTHER METHODS FOR ANALYSIS OF POLARIZED LIGHT SCATTERING

Digital image processing is a new method that has rapidly developed with the advances made in computer science [30]. First attempts to study quantitatively the morphology by digital image analysis (DIA) are reported by using DIA for PLS simulation of polymer systems [31, 32].

The technique can be explained as follows. An image of the object under study is obtained by means of light or electron microscope. The image is then converted by TV camera into video signals, digitized and transferred to a processing system, where it can be processed and relevant patterns are generated. The computation of a Fourier transformation on an image by DIA is called computer simulation of diffraction.

The difference between DIA simulation and scattering methods is of principal nature [32]. In DIA the Fourier transformation is computed for microscope images which naturally have only the intensity information. In scattering, on the other hand, both intensity and phase are involved in the optical Fourier transformation.

This can be related to optical modeling by comparing the optical transforms, for example, of spherulitic models at Hv-scattering and the relevant simulated diffraction patterns by DIA of polarizing microscope images obtained under crossed polaroids [15]. In Figure 4 is shown the computer simulated Hv-scattering pattern of a spherulite of PVF obtained by using polarizing microscope and super computer [32, 33]. As can be noted this 2-d. pattern does not coincide with the familiar clover-leaf Hv-scattering pattern obtained by PLS or optical modeling (No. 1, Fig. 1) in the physical experiment. It bears, however, an obvious resemblance to the optical transform shown in the rermark to Figure 1, differing only in the fine details of the central spot and the meridional reflections at n. 45 (n being an odd integer). The difference may be caused by several reasons. The distinguished central spot structure in the simulated pattern may result from the better resolution of the digital computer. The discrete and sequential way of computer processing might also have some effect on the pattern [34], as well as the photographic emulsion.

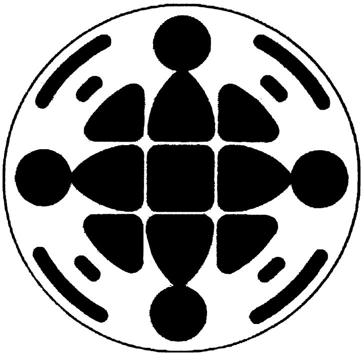

FIGURE 4 DIA simulated scattering pattern of a spherulite of poly(vinylidene fluoride) obtained by using polarizing microscope and super computer [31, 32].

One can note that both the simulated pattern (Fig. 4) and the relevant optical transform obtained without phase filters (Remark, Fig. 1) are complementary patterns to the classical Hv-scattering pattern in the sense that intensity minima and maxima change their places. This is cannonically connected to π phase shifting of light by the halves of an object [35]. An example is the apodization technique, in particular, by π step [9] used to change phase statistics with many interesting applications.

In DIA, one virtually accounts for the phase shift defined alone by the geometrical position of the scattering units. Such processing is successful but only in the case of isotropic scattering, *e.g.*, DIA patterns calculated for phase-contrast microscope images [32] are not biased.

Thus, the constraints on the additional phase shift δ to simulate entirely a real wave of the form in Eq. 1 should read:

$$\begin{array}{ll} \delta = |[\mathrm{k(rS)}] & \text{when } (\mathrm{PO}) > 0, | \\ \quad\ |[\mathrm{k(rS)} + \lambda/2] & \text{when } (\mathrm{PO}) < 0| \end{array} \tag{12}$$

It is worth considering also other methods in use for analysis of the experimental scattering [2]. Among them are the computational methods, which allow to compute the amplitude and intensity envelope of scattered light for model structures, usually on the basis of the single-particle scattering theory. It is clear that the scattering patterns and the parameters of the structures obtained by the modeling methods, both the computational methods and the optical modeling, refer exclusively to the models used in their production. Therefore their effectiveness depends on the correct approximation of the real structure by the model, which is especially important in scattering at small angles. It is recalled that small angle scattering is inherently related to larger structures (areas) which in polymer solids usually do not have regular and distinct appearance. The situation is even more complicated in the case of polarized light scattering where the method ‘‘sees’’ areas of correlation of birefringent units (optical anisotropy and/or orientation fluctuations) in the solids.

The computer simulation of diffraction where digital Fourier transform is performed over an image of the real object makes use naturally of a better approximation of the object. In view of modern techniques of image analysis, it provides new possibilities for the processing of polarized light images. But so far it can easily be related to the object parameters only in cases of objects with distinct morphology. Other methods like the correlation methods [2], are very time consuming although sometimes suggest the only solution. From the foregoing it is evident that any given object under study needs individual consideration aiming to find the best appropriate method for its study.

CONCLUDING REMARKS

The concept considered for optical modeling of polarized light scattering extends the method of the optical Fourier transforms assuming analogy between PLS from anisotropic solid polymers and non polarized light diffraction at isotropic objects, and can easily be related to other anisotropic systems as well.

Specifically, in the case of optical modeling of Hv-polarized light scattering from anisotropic samples, one has to account for the entire polarization conditions at scattering. It is necessary to introduce an additional phase difference to model adequately the action of the crossed analyzer. The constraints on the additional phase shift are determined, thus optical analogs of different morphological types in solid polymers are constructed. Their transforms are similar in appearance to the scattering patterns from real objects.

The application of the optical modeling to evaluate interparticle interference effects has shown that the optical modeling methods have potentials in coherent optics still not exhausted. An example of interaction between the optical modeling and the technique of digital image analysis of polymer systems is given. It implies that the optical modeling of PLS can inherently supply solid input data for other methods, in particular, for the computer simulation of PLS by DIA.

Acknowledgment

The author thanks Dr. M. Matsuo (Japan) for his comments on the application of digital image analysis for simulation of polarized light scattering.

References

[1] Stein, R. S. and Rhodes, M. B. (1960). *J. Appl. Phys.*, **31**, 1873.

[2] Hauden, J. (1986). In: *Optical Properties of Polymers*, Ed., Meeten, G. (Elsevier, London & New York), Chap. 2.

[3] Moneva, I. (1996). In: *Oriented Polymer Materials*, Ed., Fakirov, S. (Huethig & Wepf V.), Chap. 8, pp. 241–164.

[4] Bragg, W. L. (1939). *Nature*, **143**, 678.

[5] Taylor, C. and Lipson, H. (1964). *Optical transforms* (G. Bell & Sons Ltd., London).

[6] Lipson, H. and Taylor, C. (1966). *Progress in optics*, Ed., Wolf, E. (North Holland Publ. Co.), Vol. V.

[7] Wainstein, B., (1963). *Diffraction of X-rays at chain molecules* (Academic press USSR, Moscow), p. 178.

[8] Hosemann, R. and Bagchi, S. (1963). *Direct Analysis of Diffraction by Matter*, (NHP Co., Amsterdam).

[9] Stark, H. (1982). *Applications of Optical Fourier Transforms* (Academic Press, New York & London).

[10] Wilson, P., Krimm, S. and Stein, R. S. (1961). *J. Phys. Chem.*, **65**, 1749.

[11] Brestkin, Yu. and Ginzburg, B. (1969). *High Mol. Compounds* (*in Russian*), **AIX**, 2351.

[12] Moneva, I. (1970). *Ph.D. Thesis*, Leningrad, USSR.

[13] Moneva, I., Brestkin, Y., Ginzburg, B. and Frenkel, S. (1972). *Eur. Polym. J.*, **8**, 1033.

[14] Moneva, I., Brestkin, Y., Ginzburg, B. and Frenkel, S. (1972). *Commun. Dept. Chem. Bulg. Acad. Sci.*, **5**, 473.

[15] Moneva, I. (1996). *J. Polym. Sci.*: *Part B*: *Polym. Phys.*, **32**, 2139.

[16] Samuels, R. (1968). *J. Polym. Sci.*, A2, **6**, 1101.

[17] Daniewska, I., Hashimoto, T. and Nakai, A. (1984). *Polym. J.*, **16**, 49.

[18] Brestkin, Yu., Ginzburg, B., Moneva, I. and Frenkel, S. Ya. (1969). *Soviet Physics – Solid State*, **10**, 2471.

[19] Brestkin, Yu., Ginzburg, B. and Moneva, I. (1972). *High Mol. Compounds* (in Russian) **AIV**, p. 2222.

[20] Baranov, V. (1966). *Optika i spektroskopiya*, **21**, 610.
[21] Hood, F. I. J. M. (1969). *Proc. of the Conf. Optical instruments and techniques*, Reading (UK).
[22] Picot, C., Stein, R. S., Marchessault, R., Borch, J. and Sarko, A. (1971). *Macromolecules*, **4**, 467.
[23] Prud'homme, R. and Stein, R. S. (1973). *J. Polym. Sci. Polym. Phys. Ed.*, **11**, 1357.
[24] Wilkes, G., Mohadger, Y. and Holaday, W. (1976). *J. Polym. Sci. Polym. Phys. Ed.*, **14**, 251.
[25] van de Hulst, H. C. (1961). *Light scattering by small particles* (in Russian, Izd. In. lit., Moscow), p. 14.
[26] Yoon, D. Y. and Stein, R. S. (1974). *J. Polym. Sci. Polym. Phys. Ed.*, **12**, 735.
[27] Goodman, J. (1975). In: *Laser Speckle and Related Phenomena*, Ed., Dainty, J. (Springer V., Berlin).
[28] Dudderar, T. and Simpkins, P. (1982). *Optical engineering*, **21**, 396.
[29] Holoubek, J. and Sedlacek, B. (1980). *J. Polym. Sci. Polym. Phys. Ed.*, **18**, 265.
[30] Harlow, C., Dwyer, S. and Lodwick, G. (1976). In: *Topics of Applied Physics*, Ed. Rosenfeld, A. (Springer Verlag), **11**, 70.
[31] Tanaka, H., Hayashi, T. and Nishi, T. (1986). *J. Appl. Phys.*, **59**, 653.
[32] Tanaka, H., Hayashi, T. and Nishi, T. (1986). *J. Appl. Phys.*, **59**, 3627.
[33] *Second Circular of IUPAC 32nd Int. Symposium on Macromolecules* (Kyoto, Japan, 1988).
[34] Hopkins, H. H. (1990). *Private communication* (Reading).
[35] Born, M. and Wolf, E. (1970). *Principles of optics*, 2nd edn., (in Russian), (Nauka, Moscow), (a) p. 761 (b) p. 452.